Fig. 1 Two tracks (solid lines) identification using three different "views" of the detection planes. The third detection plane ("V view") allowes to reject spurious tracks (dashed lines).
Fig. 2 The "lef-right ambiguity" verification using a staggered plane shifted by 1/4 of the cell width. The true track (solid line) is distinguished from the spourious tracks (dashed lines).
Fig. 3 Cross section of the T3 prototype detection plane. The anode (A), cathode (C) and field shaping wires (F) are shown.
Fig. 4 The drift chamber prototype module under construction.
Fig. 5 Schematic diagram of the test run set up (see text for details).
Fig. 6 Cross section of the X0, X1, X2 detection planes. Triangles and circles indicate the anode and cathode wires, respectively. Reconstructed tracks are also shown (thin solid lines).
Fig. 7 Efficiency of the drift chamber prototype as a function of the anode-cathode high voltage difference for three different gas mixtures.
Fig. 8 The event distributions per time bin dN/dt (left column) and the integrals of these distributions (right column) for the wire number 12. $75\% Ar + 25\% C_4H_{10}$ gas mixture has been used.
Fig. 9 Reconstructed tracks (thin solid lines) using the signals recorded by the anode number sequences 12-12-12 (left panel) and 13-12-13 (right panel). The triangles and circles denote the anode and cathode wires, respectively.
Fig. 10 Calibration integral for t_{max}=100 nsec (left panel) and distribution of the deviation Δ (see eq. 2) for the anode number sequence 12-12-12 (right-upper panel). The distribution of the deviation Δ for the anode sequence 13-12-13 (right-lower panel).
Fig. 11 Same as Fig. 10 but for t_{max}=300 nsec.
Fig. 12 Same as Fig. 10 but for t_{max}=145 nsec.
Fig. 13 Position resolution for $75\% Ar + 25\% C_4H_{10}$ gas mixture.
Fig. 14 Position resolution for $67\% Ar + 33\% C_4H_{10}$ gas mixture.
Fig. 15 Single module of the T3 detector.
Fig. 16 The T3 drift chamber detector at the forward spectrometer of the BRAHMS experiment set up.

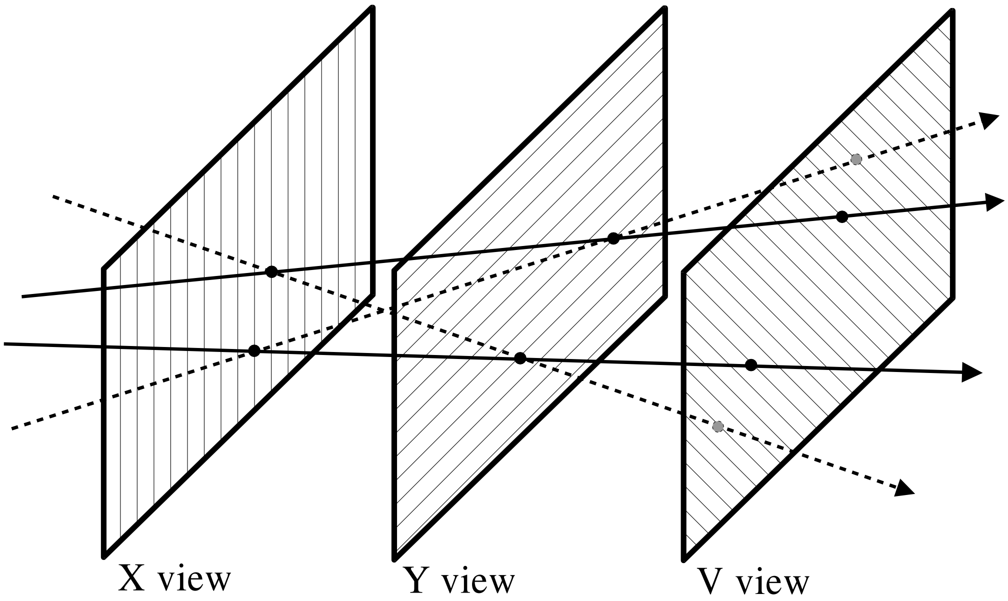

Fig. 1 Two tracks (solid lines) identification using three different "views" of the detection planes. The third detection plane ("V view") allowes to reject spurious tracks (dashed lines).

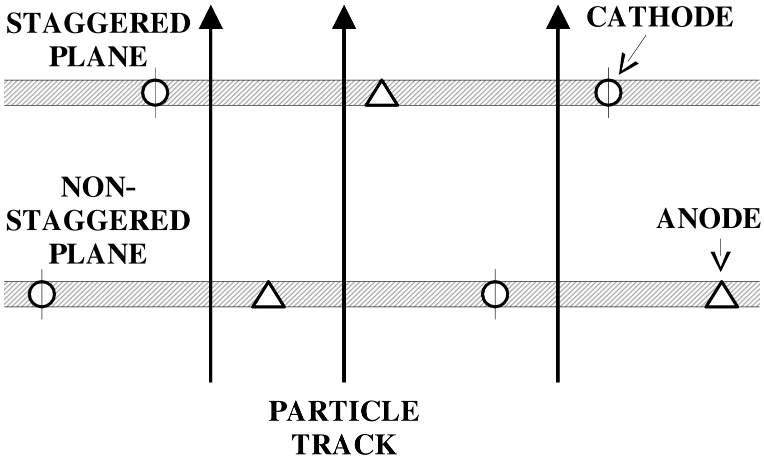

Fig. 2 The "lef-right ambiguity" verification using a staggered plane shifted by 1/4 of the cell width. The true track (solid line) is distinguished from the spourious tracks (dashed lines).

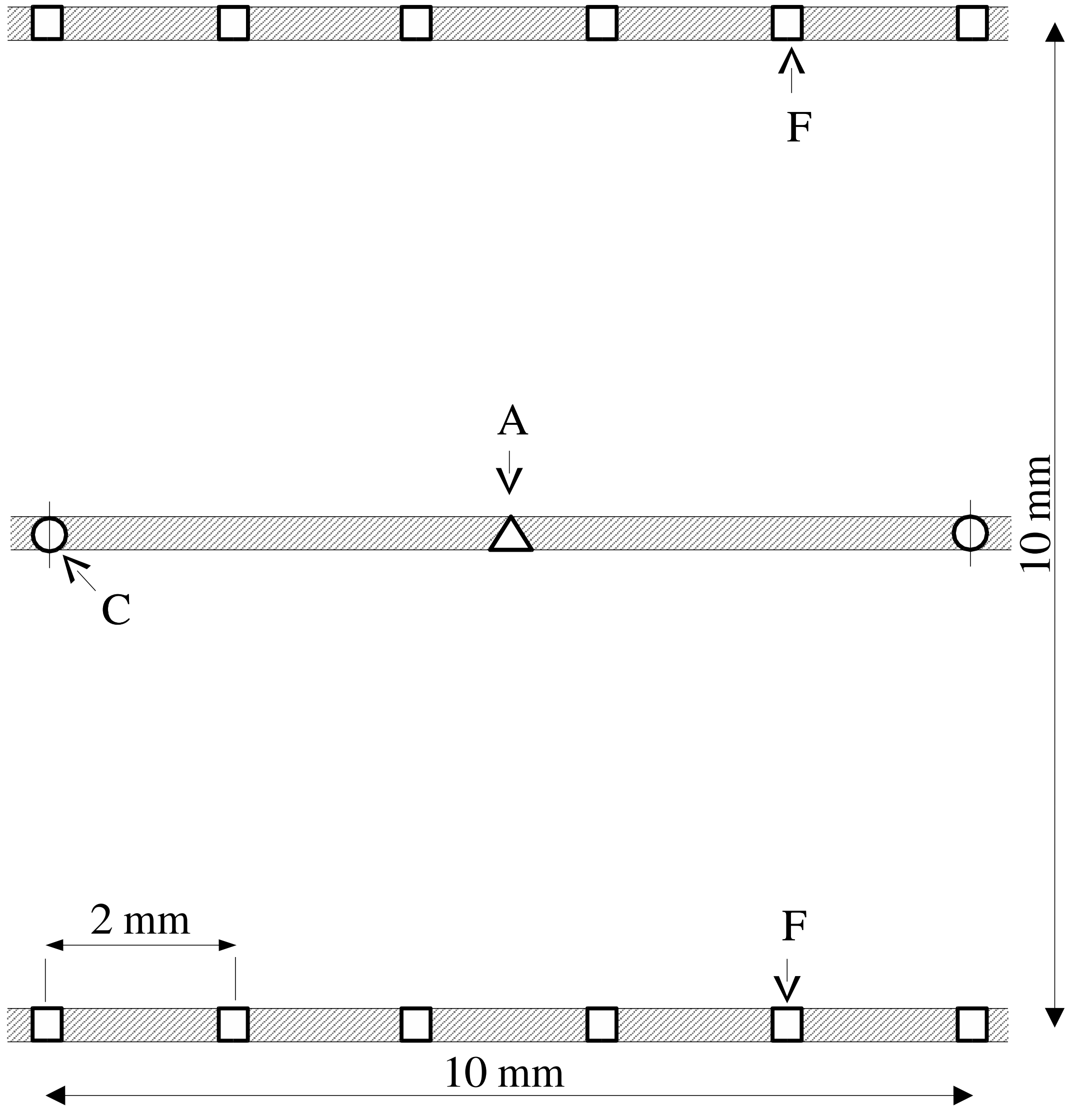

Fig. 3 Cross section of the T3 prototype detection planes. The anode (A), cathode (C) and field shaping wires (F) are shown.

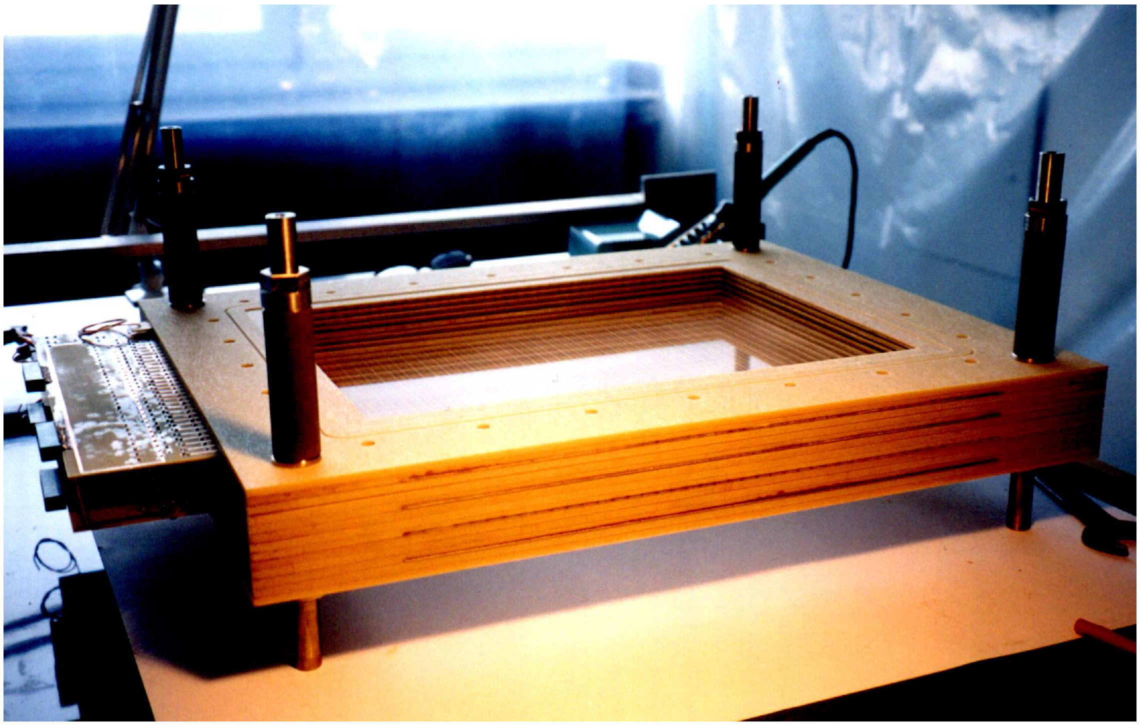

Fig. 4 The prototype module under construction.

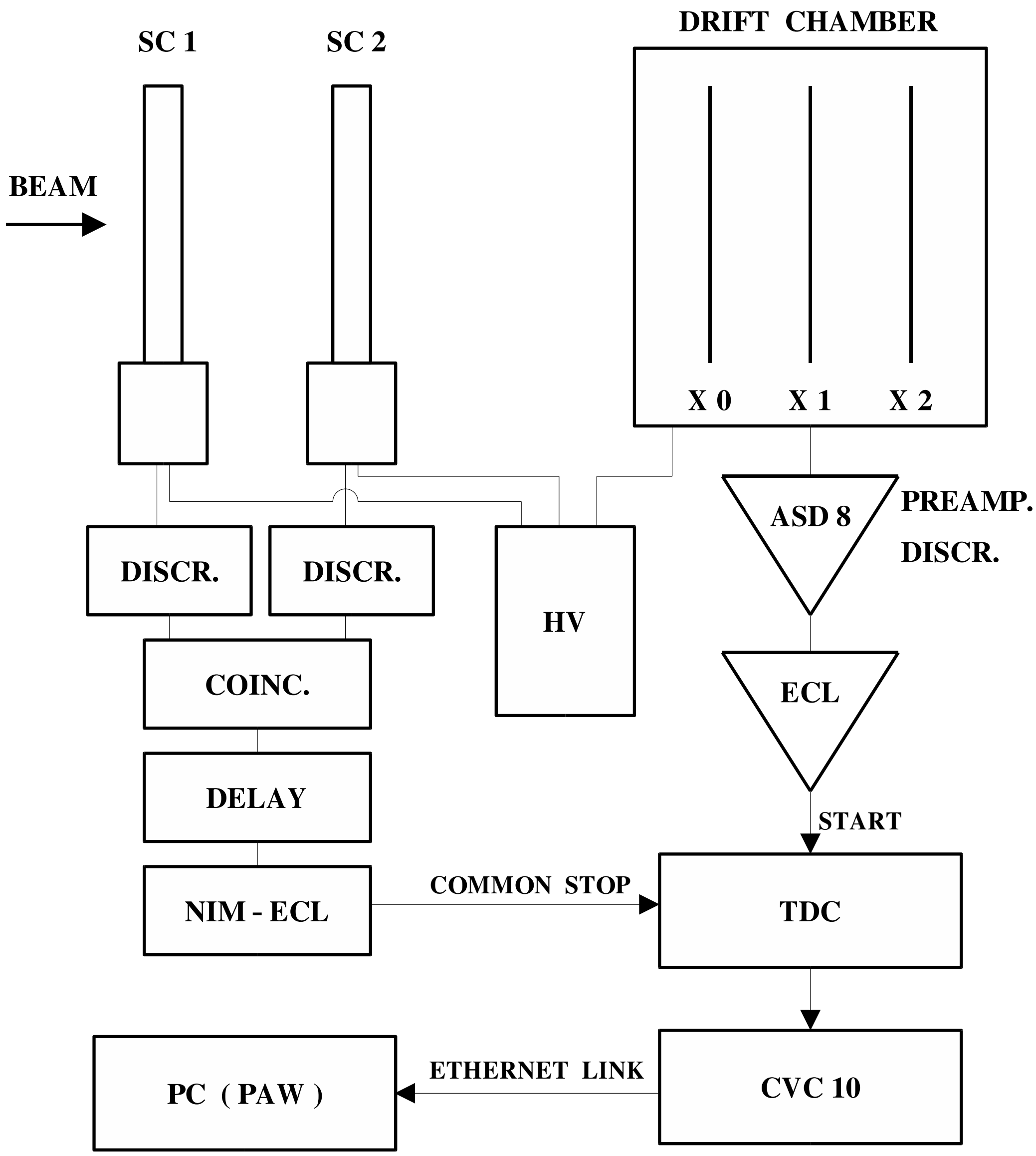

Fig. 5 Shematic diagram of the test run set up (see text for details).

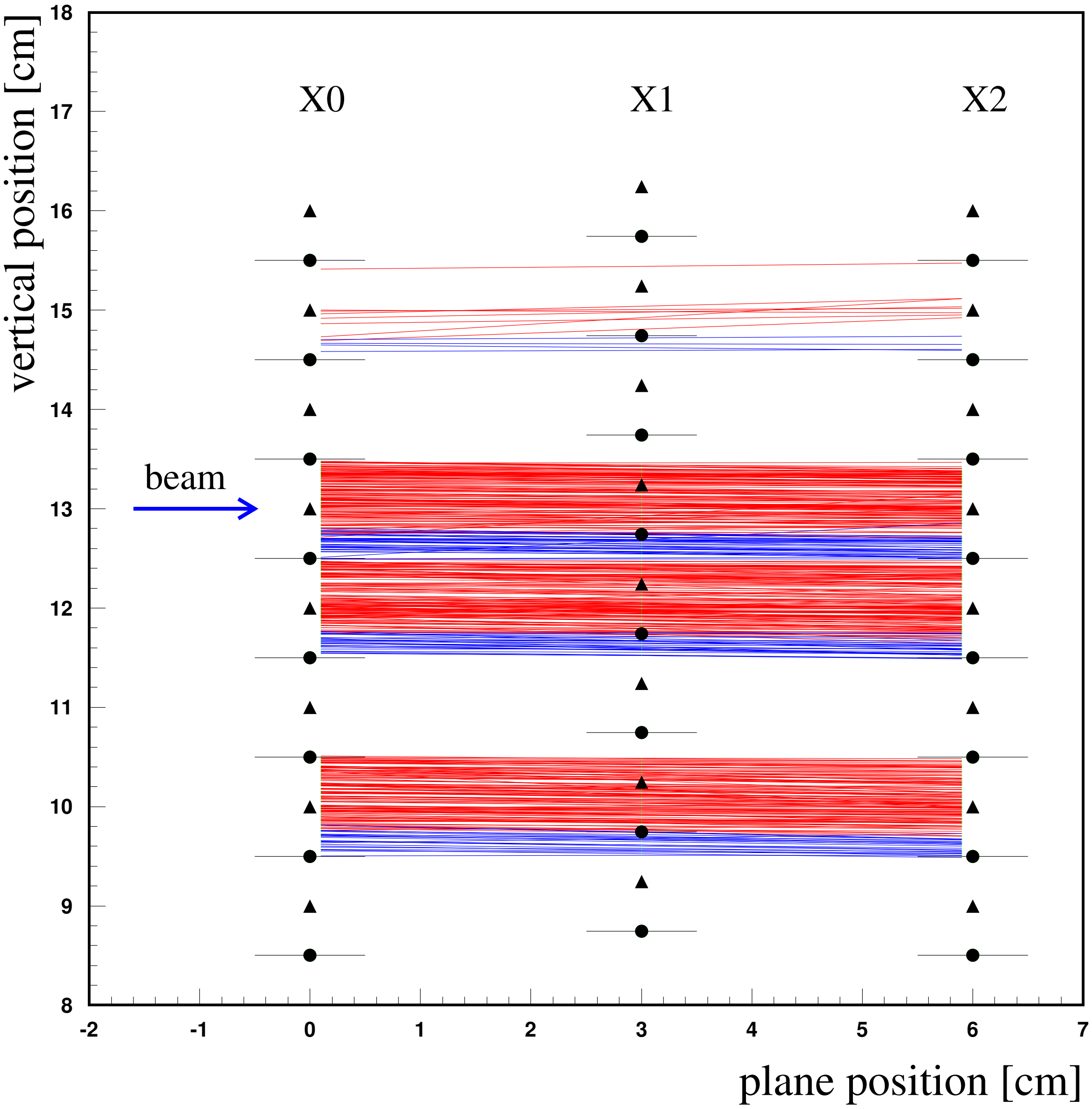

Fig. 6 Cross section of the X0, X1, X2 detection planes. Triangles and circles indicate the anode and cathode wires, respectively. Reconstructed tracks are also shown (thin solid lines).

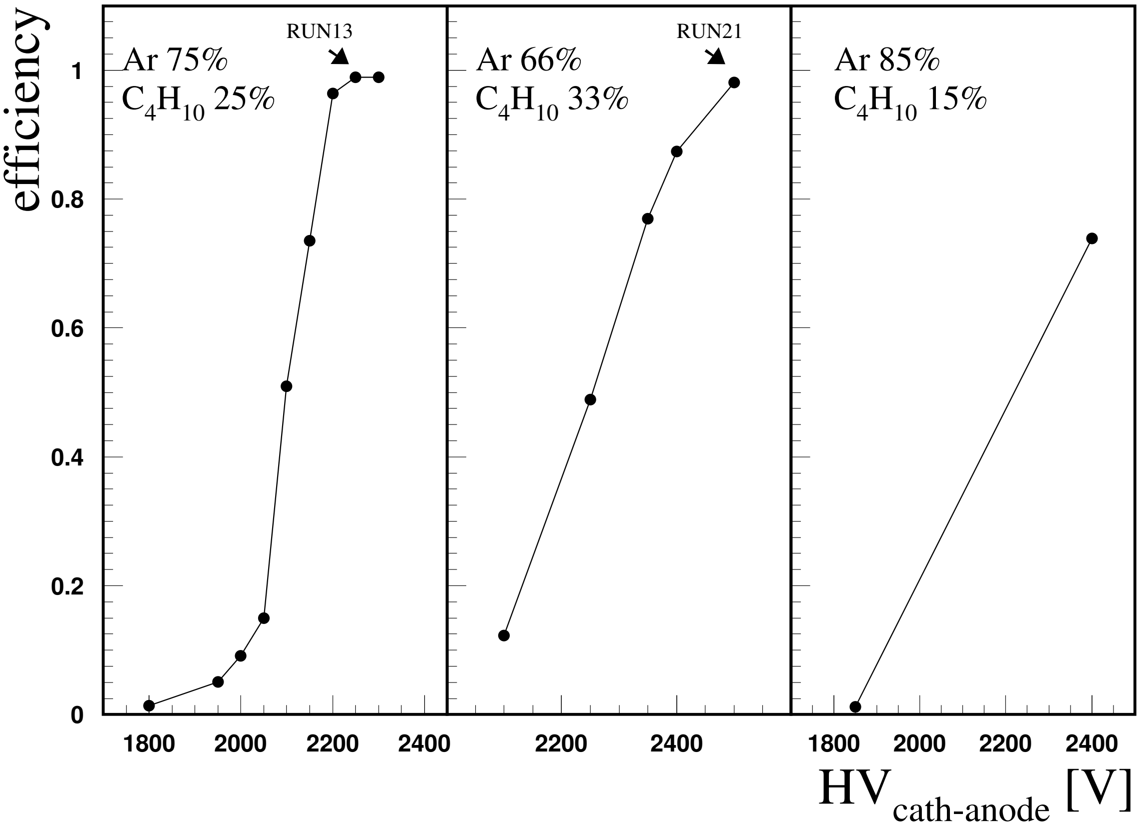

Fig. 7 Efficiency of the drift chamber prototype as a function of the anode-cathode high voltage difference for three different gas mixtures.

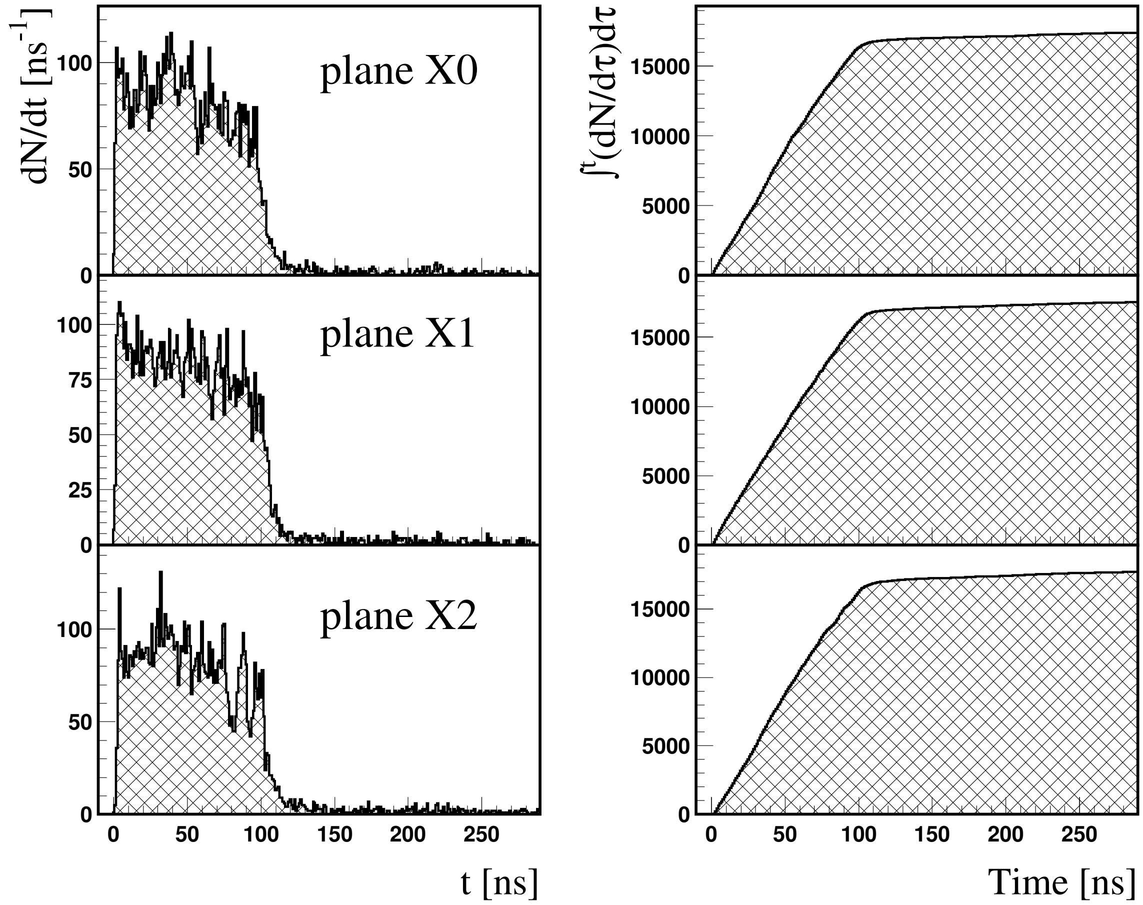

Fig. 8 The event distributions per time bin dN/dt (left column) and the integrals of these distributions (right column) for the wire number 12. $75\% Ar + 25\% C_4H_{10}$ gas mixture has been used.

0 50 100 150 200 250 0 50 100 150 200 250

0 50 100 150 200 250 0 50 100 150 200 250

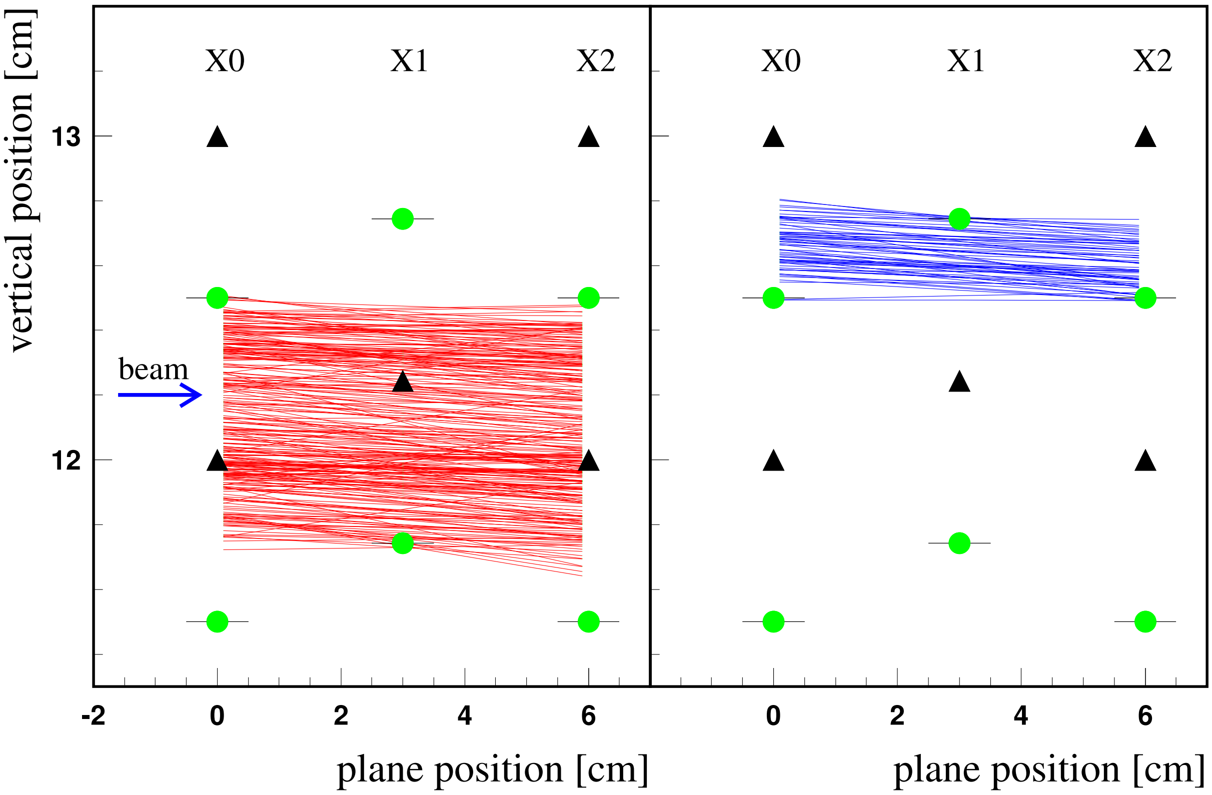

Fig. 9 Reconstructed tracks (thin solid lines) using the signals recorded by the anode number sequences 12-12-12 (left panel) and 13-12-13 (right panel). The triangles and circles denote the anode and cathode wires, respectively.

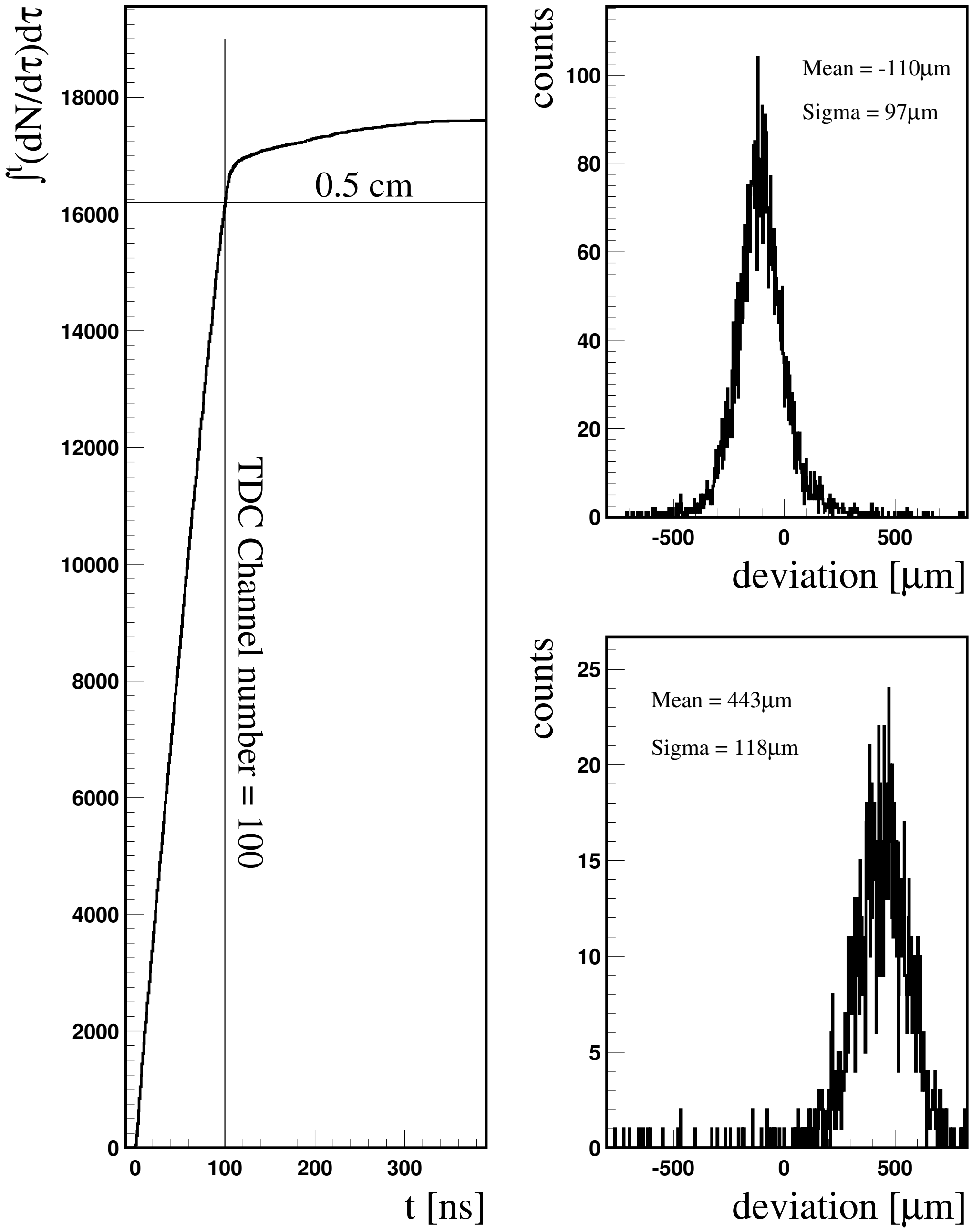

Fig. 10 Calibration integral for t_{max}=100 nsec (left panel) and distribution of the deviation Δ (see eq. 2) for the anode number sequence 12-12-12 (right-upper panel). The distribution of the deviation Δ for the anode sequence 13-12-13 (right-lower panel).

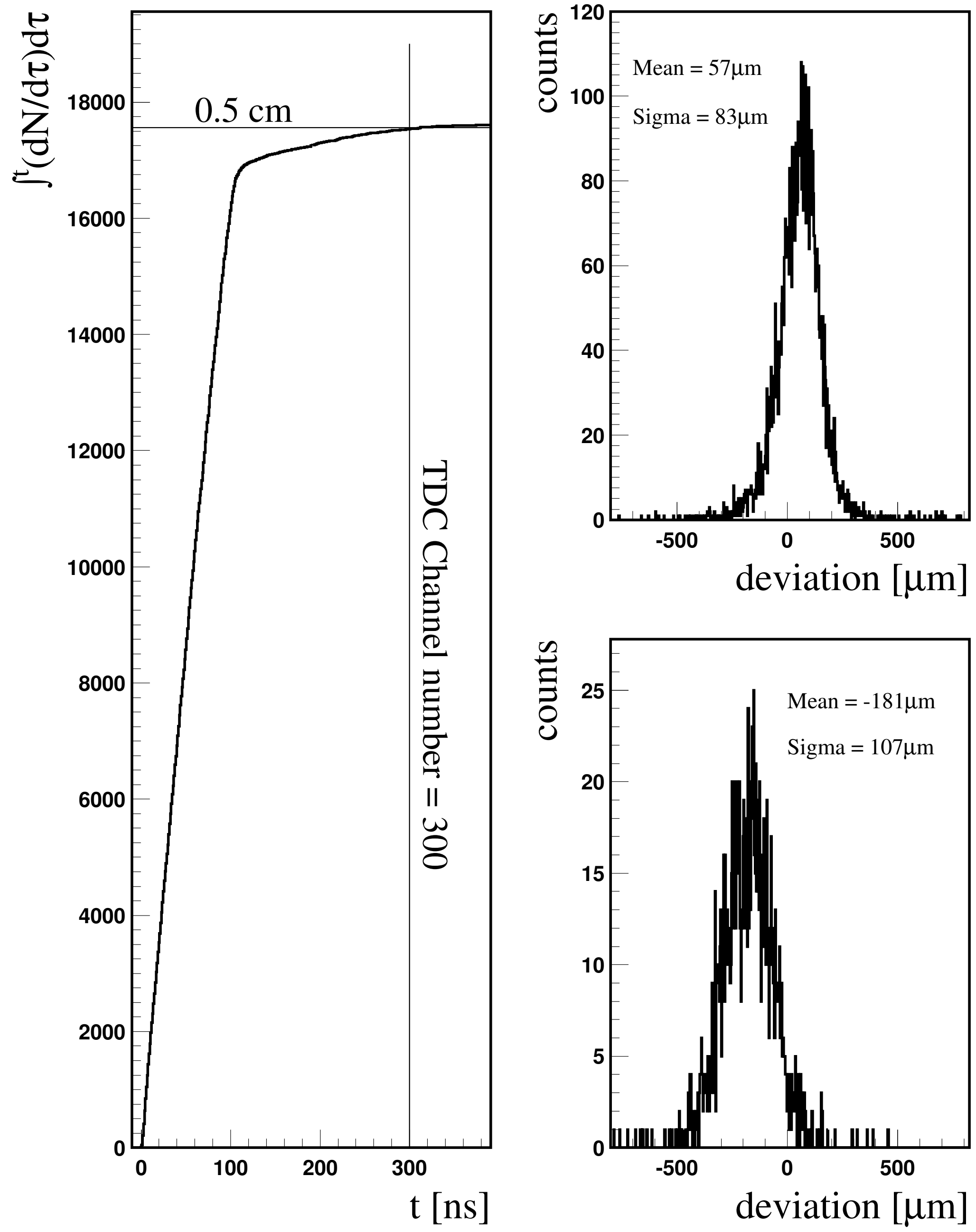

Fig. 11 Same as Fig. 10 but for t_{max}=300 nsec.

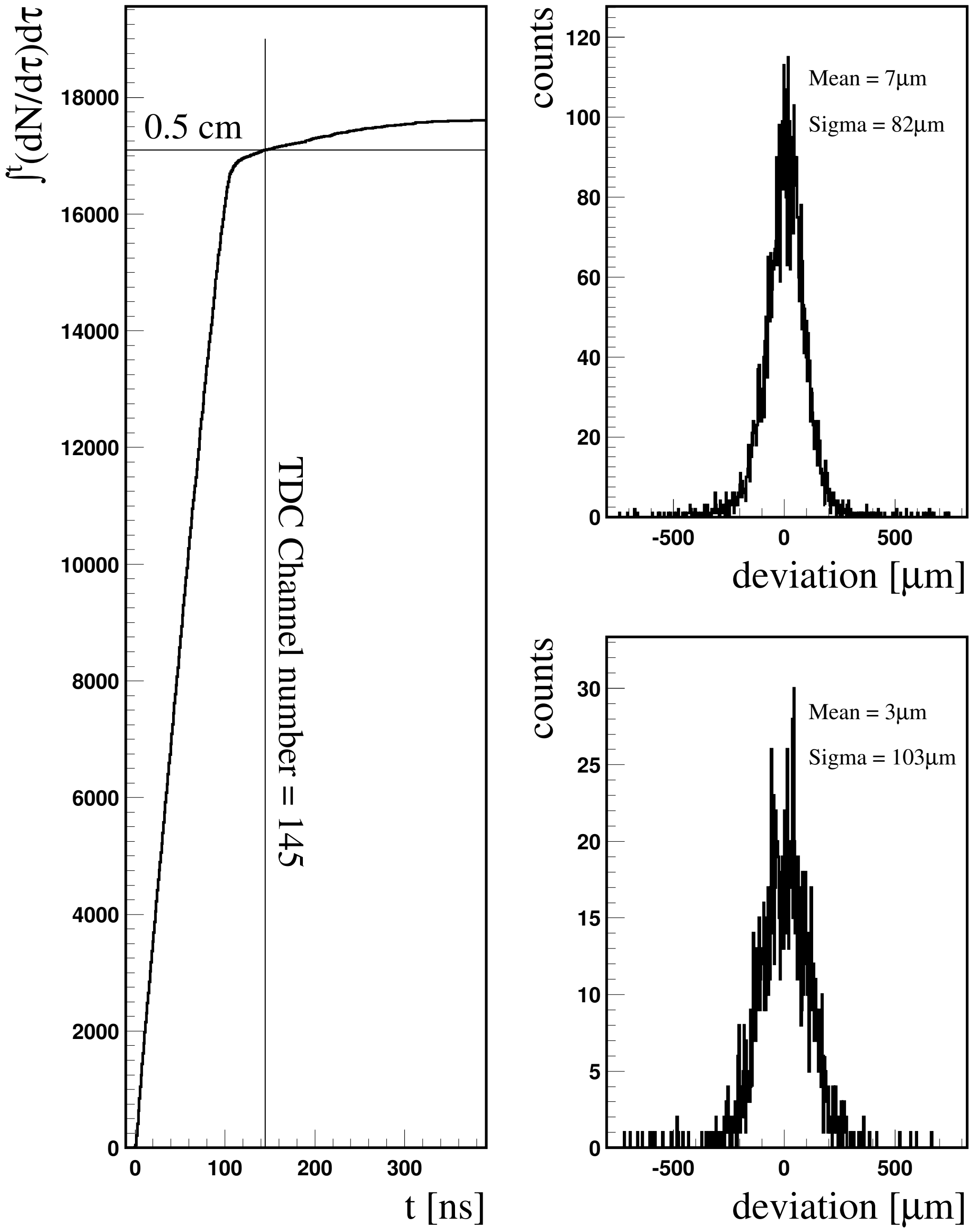

Fig. 12 Same as Fig. 10 but for t_{max}=145 nsec.

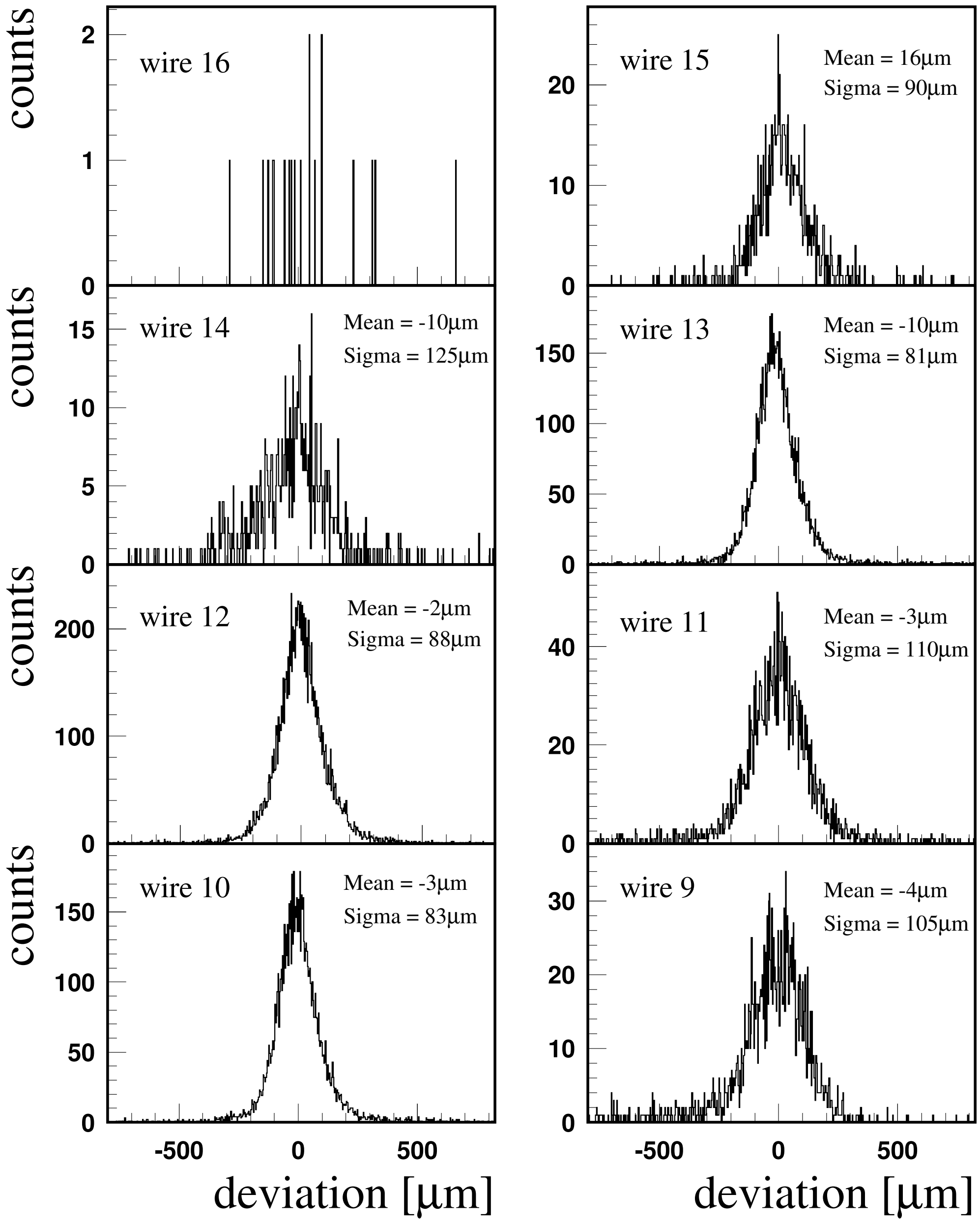

Fig. 13 Position resolution for $75\% Ar + 25\% C_4H_{10}$ gas mixture.

-500 0 500 -500 0 500

-500 0 500 -500 0 500

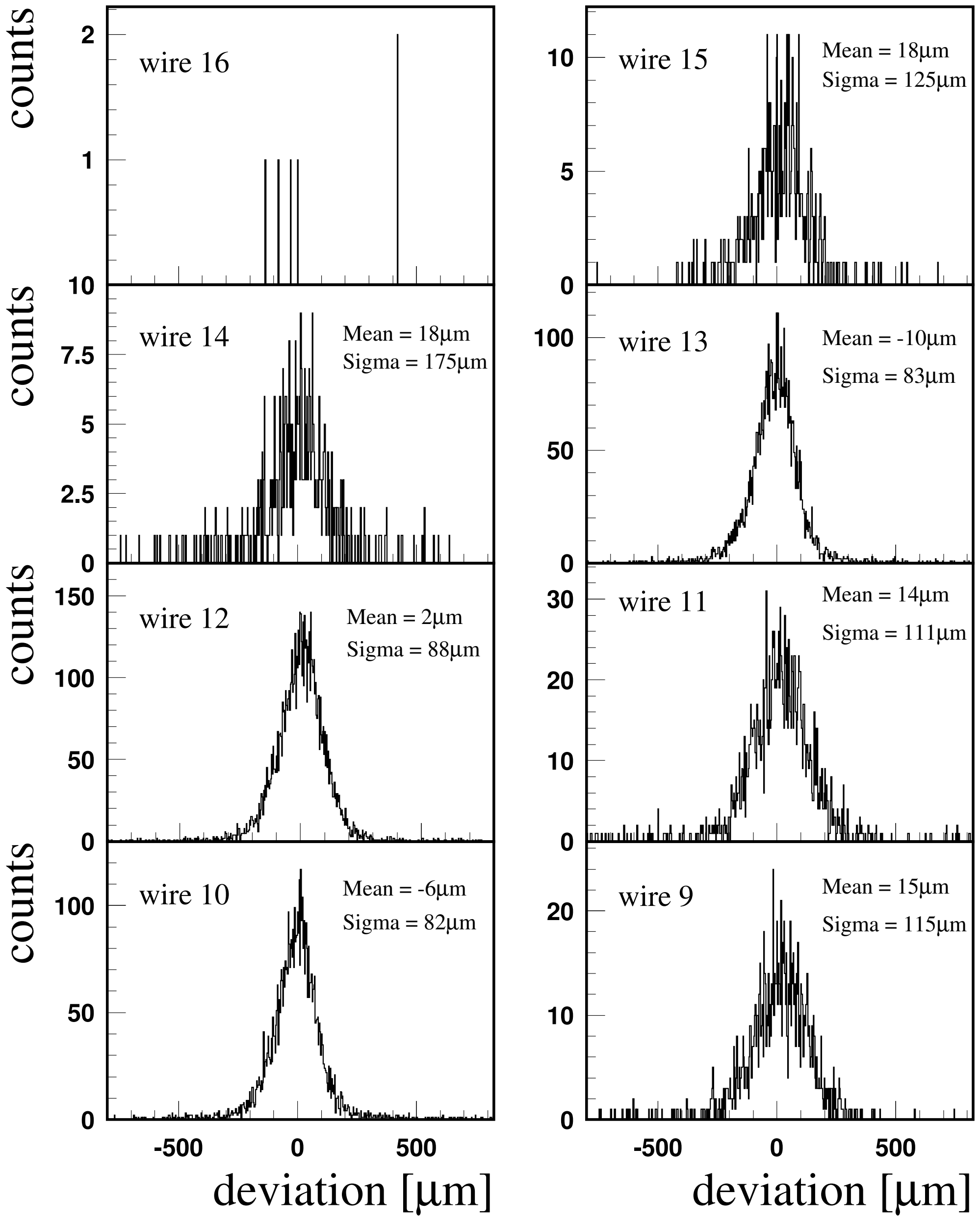

Fig. 14 Position resolution for $67\% Ar + 33\% C_4H_{10}$ gas mixture

-500 0 500 -500 0 500

-500 0 500 -500 0 500

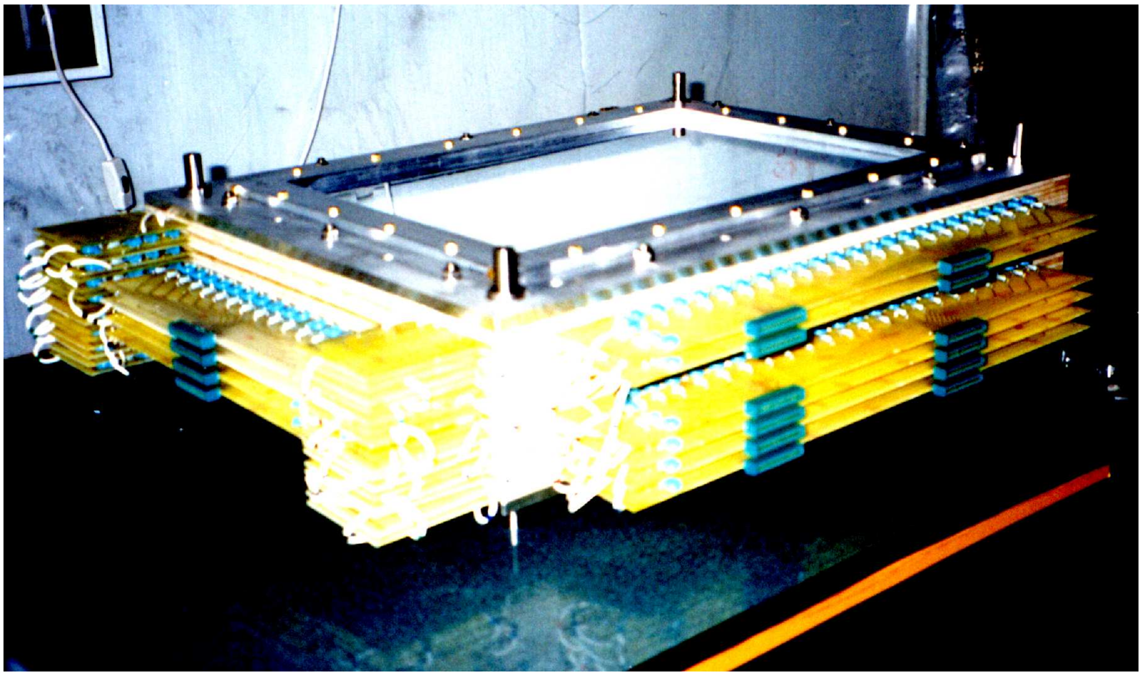

Fig. 15 Single module of the T3 detector.

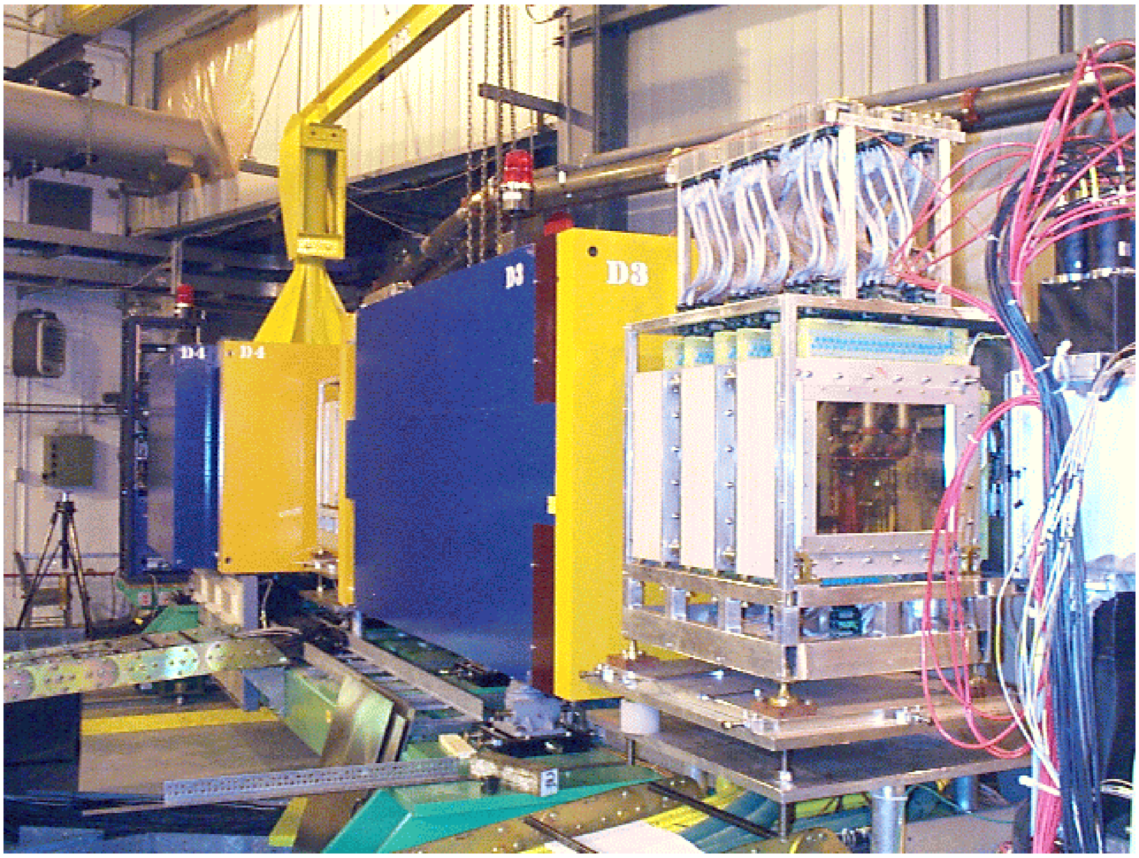

Fig. 16 The assembled T3 detector.